Published OnlineFirst October 28, 2016; DOI: 10.1158/0008-5472.CAN-15-3032

Therapeutics, Targets, and Chemical Biology

Cancer Research

Phospholipase D1 Acts through Akt/TopBP1 and RB1 to Regulate the E2F1-Dependent Apoptotic Program in Cancer Cells

Dong Woo Kang[1,2], Shin Wha Lee[1,3], Won Chan Hwang[2], Bo Hui Lee[4], Yong-Seok Choi[4], Young-Ah Suh[1], Kang-Yell Choi[5,6], and Do Sik Min[2,6,7]

Abstract

The RB1/E2F1 signaling pathway is frequently deregulated in colorectal cancer and has been suggested to intersect with Wnt/β-catenin and PI3K/Akt pathways, but molecular evidence for this link is lacking. In this study, we demonstrate that phospholipase D1 (PLD1), a transcriptional target of β-catenin/TCF4, orchestrates functional interactions between these pathways during intestinal tumor development. Overexpression of PLD1 in intestinal epithelial cells protected cells from apoptosis induced by PLD1 ablation in the $Apc^{min/+}$ mouse model of intestinal tumorigenesis. Mechanistic investigations revealed that genetic and pharmacologic targeting of PLD1 promote the E2F1-dependent apoptotic program via both miR-192/4465–mediated downregulation of RB1 and inhibition of Akt–TopBP1 pathways. Moreover, the miRNA–RB1 axis and Akt pathway also contributed to the PLD1-mediated self-renewal capacity of colon cancer–initiating cells. Finally, PLD1-driven E2F1 target gene expression positively correlated with tumor stage in patients with colorectal cancer. Overall, our findings suggest that PLD1 mediates cross-talk between multiple major signaling pathways to promote the survival and malignancy of colon cancer cells and may therefore represent an ideal signaling node for therapeutic targeting. *Cancer Res; 77(1); 142–52. ©2016 AACR.*

Introduction

Deregulation of the retinoblastoma tumor suppressor, RB1, and E2F pathway is a common feature of many cancers (1). RB1 mainly exerts its tumor-suppressive effects by restraining the activity of E2F transcription factor, which subsequently regulates cellular proliferation and apoptosis depending on the cellular contexts (2). Although RB1 is inactivated in a wide variety of human cancers, loss or mutations of the *RB1* gene are rare, and the *RB1* gene is frequently overexpressed in colorectal cancer (3), which is linked to the antiapoptotic function of the protein. However, the mechanisms by which RB1 regulates apoptosis are yet to be fully elucidated. Although recent studies suggest that there is a cross-talk of the RB1/E2F1 pathway with the Wnt signaling pathways in colorectal cancer (4, 5), the mechanism underlying their functional interaction remains elusive. Most human colorectal cancers involve somatic mutations in the adenomatous polyposis coli (APC) tumor suppressor gene, which leads to the activation of Wnt signaling via stabilization and nuclear accumulation of β-catenin and its interaction with TCF transcription factor and subsequent transcriptional activation of Wnt target genes (6). E2F1 has been identified as a negative regulator of β-catenin/TCF-dependent transcription (4). Although a recent study attributed the retention of RB1 function in colorectal cancer cells to its ability to repress E2F-1–dependent inactivation of β-catenin signaling (7), little is known about the molecular mechanism linking these entangled pathways in colorectal cancer. The expression of RB1 can promote cell survival through repression of E2F-driven apoptosis (8). Thus, the interplay between RB1/E2F1 and Wnt/β-catenin signaling pathways might be even more complex than originally thought. Accordingly, identification of critical effectors regulating the multifaceted cross-talk between signaling pathways will lead to the nomination of new candidates for creation of targeted therapies useful to colorectal cancer management. We recently demonstrated that phospholipase D1 (*PLD1*) as a new transcriptional target of β-catenin/TCF4 promotes Wnt signaling (9, 10), revealing bidirectional cross-talk between the PLD1 and Wnt/β-catenin pathways. In addition, targeting of *PLD1* attenuates intestinal tumorigenesis by suppressing β-catenin signaling (11). PLD hydrolyzes phosphatidylcholine to generate bioactive lipid phosphatidic acid (PA) and is upregulated in various human cancers, including colorectal cancer (12). Although PLD has been implicated in many survival and proliferation signals (13), the molecular mechanisms linking RB1/E2F1 and the PLD1 pathway in

[1]Institute of Innovative Cancer Research, Asan Medical Center, University of Ulsan College of Medicine, Seoul, Republic of Korea. [2]Department of Molecular Biology, Pusan National University, Busan, Republic of Korea. [3]Department of Obstetrics and Gynecology, Asan Medical Center, University of Ulsan College of Medicine, Seoul, Republic of Korea. [4]Department of Statistics, College of Natural Science, Pusan National University, Busan, Republic of Korea. [5]Department of Biotechnology, College of Life Science and Biotechnology, Yonsei University, Seoul, Republic of Korea. [6]Translational Research Center for Protein Function Control, Yonsei University, Seoul, Republic of Korea. [7]Genetic Engineering Institute, Pusan National University, Busan, Republic of Korea.

Note: Supplementary data for this article are available at Cancer Research Online (http://cancerres.aacrjournals.org/).

D.W. Kang and S.W. Lee contributed equally to this article.

Corresponding Author: Do Sik Min, Department of Molecular Biology, Pusan National University, 30 Jangjeon-dong, Geumjeonggu, Busan 609-735, Republic of Korea (South). Phone: 82-51-510-3682; Fax: 82-51-513-9258; E-mail: minds@pusan.ac.kr

doi: 10.1158/0008-5472.CAN-15-3032

Published OnlineFirst October 28, 2016; DOI: 10.1158/0008-5472.CAN-15-3032

colorectal cancer have not been addressed. As the RB1/E2F1, PI3K/Akt, and Wnt/β-catenin pathways intersect in colorectal cancer, we investigated whether PLD1 acts as a modulator of functional interaction among the pathways in intestinal tumorigenesis.

Materials and Methods

Mice

Apc$^{min/+}$*Pld1*$^{-/-}$ and *Apc*$^{min/+}$*Pld1*^{Tg} mice were generated as described previously (11). *Apc*$^{Min/+}$*Pld1*$^{-/-}$*Pld1*^{Tg} mice were generated by interbreeding mice carrying *Pld1*^{Tg} with *Apc*$^{Min/+}$*Pld1*$^{-/-}$ mice. An azoxymethane (AOM)/dextran sodium sulfate (DSS)–induced mice were treated with 10 mg/kg PLD1 inhibitor (VU0155069, Cayman Chemical) as described previously (11). Animal studies were approved by the Institutional Animal Care Committee of Pusan National University (Busan, Republic of Korea).

Human primary tumor samples and tissue microarray

Fifty-five human colon tumor and adjacent normal tissues for q-PCR analysis were obtained from Pusan National University Hospital (Busan, Republic of Korea), a member of the National Biobank of Korea, which is supported by the Ministry of Health and Welfare. All samples derived from the National Biobank of Korea were obtained with informed consent under Institutional Review Board–approved protocols. For immunohistochemical analysis, tissue microarray (TMA) slides were purchased from SuperBioChips (CDA2, CDA3, and CD4) and US Biomax (CC05-01-002). Each array includes more than 178 cases of normal, reactive, premalignant, and malignant tissues of the colon (various grades and stages). Overall survival was calculated from the date of treatment start to the date of death. Survival curves were constructed using the Kaplan–Meier methodology. Log-rank tests were used to assess differences in tumor characteristics.

Histology and IHC

Anti-NOXA (Imgenex), anti-RB1, anti-p-Akt, anti-p27KIP1, and anti-Bim antibodies (Santa Cruz Biotechnology) were used as the primary antibodies. The anti-PLD1 antibody was generated as described previously (14).

Cell lines

HCT116 p53$^{+/+}$ and p53$^{-/-}$ isogenic cell lines were kindly gifted by Dr. Bert Vogelstein (Johns Hopkins University, Baltimore. MD). MEFs from *E2F1*$^{+/+}$ and *E2F1*$^{-/-}$ mice were kindly provided by Dr. Han Woong Lee (Yonsei University, Seoul, South Korea). The human colorectal cancer cells: SW480 (ATCC CCL-228, passage number 04 - 18) and DLD1 (ATCC CCL-221, passage number 03 - 17) were obtained from the ATCC. Cell lines purchased from ATCC were analyzed by STR profiling. Tumorspheres were grown in B27 (Invitrogen) supplemented with 20 μg/mL bFGF and 20 μg/mL EGF (Sigma), and penicillin/streptomycin on ultra-low attachment culture dishes (Corning), as a sphere culture condition.

Apoptosis assay

Apoptotic cell death was measured by APC-conjugated Anti-Annexin V Apoptosis Detection Kit I (BD Biosciences). The terminal deoxynucleotidyl transferase–mediated dUTP nick end labeling (TUNEL) assay was performed using *In Situ* Cell Death Detection Kit, POD (Roche), according to the manufacturer's protocol.

Immunoprecipitation and Western blotting

Cell lysates were analyzed by immunoprecipitation and/or immunoblotting as described previously (11). Enhanced chemiluminescence was used for detection of the signal. The following antibodies were used: anti-α-tubulin, anti-c-Myc, anti-RB1, anti-phospho-RB1, anti-Bim, anti-p27KIP1, anti-p73, anti-HA, anti-mouse-IgG, and anti-rabbit-IgG (Santa Cruz Biotechnology); anti-NOXA (Thermo Fisher Scientific); TopBP1 (Abnova); anti-E2F1, anti-FLAG, and anti-phospho-serine (Sigma); anti-active caspase-3, anti-phospho-Akt, and anti-Akt1 (Cell Signaling Technology).

FACS and flow cytometry

The phycoerythrin (PE)-conjugated anti-CD133 (Miltenyi Biotec) or allophycocyanin-conjugated anti-CD44 (BD Biosciences) antibodies were used for FACS analysis. To obtain CD133^{+}CD44^{+} or CD133^{-}CD44^{-} cells, xenografted DLD1 tumor cells stained with PE-conjugated anti-CD133 and allophycocyanin-conjugated anti-CD44 antibody (both 1:40) were subjected to cell sorting performed by the FACS.

In vitro limiting dilution assays

To determine the number of sphere-forming units, *in vitro* limiting dilution assays were performed as described previously (11, 15).

mRNA microarray analysis

Microarray analysis was carried out by Macrogen Inc. Briefly, biotinylated complementary RNAs were amplified and purified using an Illumina RNA Amplification Kit (Ambion) according to the manufacturer's instructions. Labeled cRNA samples were hybridized to each HumanHT-12 expression v.4 bead array for 16 to 18 hours at 58°C, according to the manufacturer's instructions (Illumina). Detection of array signal was carried out using FluoroLink streptavidin-Cy3 (GE Healthcare Bio-Sciences). Arrays were scanned with an Illumina BeadArray Reader confocal scanner, and the scanned images were analyzed using an Illumina BeadStudio v3.1.3 software (Gene Expression Module v3.3.8). All data normalization and selection of fold-changed probes were performed using GeneSpringGX 7.3 (Agilent Technologies). We performed data transformation (set measurements <0.01–0.01) and per chip (normalize to 75th percentile) normalization. Probes that were changed not less than 1.25-fold and 2-fold of ratio in shPLD1/shCTRL and shPLD1-shE2F1/shPLD1 groups were selected and considered as differentially expressed probes.

The GEO accession numbers

The mRNA and miRNA microarray data reported in this article are GSE55724 and GSE55771, respectively.

Primer sets for qRT-PCR, chromatin immunoprecipitation assay, and mice genotype

The primer sets are listed in Supplementary Tables S1–S3.

Statistical analysis

Data were analyzed using the paired *t* test or ANOVA test, and correlation coefficients were calculated using Spearman *r*.

Published OnlineFirst October 28, 2016; DOI: 10.1158/0008-5472.CAN-15-3032

Colorectal cancer patient survival probability, defined as the time from colon resection to death or the date of last follow-up, was analyzed using Kaplan–Meier method, and differences were evaluated using log-rank test. Immunohistochemical staining results were analyzed using χ^2 test. Statistical analysis was performed using Origin 8.0 and GraphPad Prism 5.0.

For detailed information, please refer to the Supplementary Materials and Methods.

Results

PLD1 plays a crucial role in the regulation of apoptosis during intestinal tumor development

Recently, we reported that intestinal epithelial cell (IEC)-specific PLD1 overexpression in $Apc^{Min/+}$ mice accelerates intestinal tumorigenesis with increased proliferation and β-catenin level, compared with $Apc^{Min/+}$ mice, whereas loss of PLD1 in $Apc^{Min/+}$ mice suppresses the intestinal tumorigenesis based on tumor number, tumor size, and survival probability (11). Evasion of apoptosis is a hallmark of cancer and contributes both to the development of the tumor and the refractory nature of tumors to treatment (16). Although PLD1 is known to protect apoptosis *in vitro* (17, 18), the role of PLD1 in the regulation of apoptosis *in vivo* mice models has not yet been described. Thus, we examined whether PLD1 regulates apoptotic function *in vivo* tumor model using $Apc^{Min/+}$ mice. The proportions of TUNEL-positive apoptotic cells in intestinal tumors of 14-, 16-, and 20-week-old $Apc^{Min/+}Pld1^{-/-}$ mice were remarkably higher than in $Apc^{Min/+}$ control mice (Fig. 1A). IEC-specific PLD1 overexpression in $Apc^{Min/+}Pld1^{-/-}$ mice ($Apc^{Min/+}Pld1^{-/-}Pld1^{Tg}$) significantly reduced the proportions of the apoptotic cells induced in $Apc^{Min/+}Pld1^{-/-}$ mice (Fig. 1A). In accordance with the result, the mortality of $Apc^{Min/+}Pld1^{-/-}Pld1^{Tg}$ mice was significantly increased relative to $Apc^{Min/+}Pld1^{-/-}$ mice, whereas $Apc^{Min/+}Pld1^{-/-}$ mice exhibit an increased survival rate compared with $Apc^{Min/+}$ littermate controls (Fig. 1B). Serum deprivation under tumor microenvironment simulates the harsh growth environments encountered by neoplastic cells prior to vascularization and restoration of nutrient supply within the tumor mass. PLD1 depletion increased apoptosis of the HCT116 cells in the presence of 0%, 0.5%, or 1% of serum but not 3% or 10% of serum (Fig. 1C). Ectopic expression of PLD1 in PLD1-depleted cells protected the apoptosis induced by serum deprivation (Fig. 1C). These results are comparable with those of $Apc^{Min/+}$mice. Moreover, PLD1 inhibition also showed that the results are comparable with those of PLD1 depletion (Supplementary Fig. S1A). The serum deprivation significantly increased the formation of PA, a product of PLD activity, which was suppressed by PLD1 inhibitor (VU0155069; Supplementary Fig. S1B), suggesting that serum deprivation–generated PA may prevent cancer cells from apoptosis. Taken together, these results indicate that PLD1 plays a crucial role in the modulation of apoptosis *in vivo* and *in vitro* under tumor microenvironment.

PLD1 inactivation–induced apoptosis is associated with downregulation of RB1

The antiapoptotic survival signals generated by PLD are known to be mediated, at least in part, by suppression of the p53 response pathway (19, 20). Thus, we examined the role of p53 in PLD1-mediated apoptotic regulation using HCT116 p53-positive and -negative isogenic cell lines. Contrary to our expectation, depletion and inhibition of PLD1 induced apoptosis independent of p53 (Fig. 2A). Recently, we performed an mRNA microarray in DLD1 and HCT116 cells under serum-deprived conditions (11). The genes commonly up- or down-regulated in PLD1 inhibitor–treated or PLD1-depleted cells were visualized by scatter diagrams (Fig. 2B). PLD1 inactivation increased expression of the positive regulators of apoptosis (Bim, p73, NOXA, p27KIP1, DR5, Cyp26b1, p14ARF, and Nr4A3) and endoplasmic reticulum stress (CHOP, GCLC, Mif1, and Sos2), but decreased the expression of *RB1* and cell cycle progression–related genes (Fig. 2B; Supplementary Fig. S2). PLD1 inhibition suppressed the protein level of endogenous RB1 in HCT116 cells, whereas PLD1 inhibition–induced apoptosis under serum starvation was prevented by ectopic expression of RB1 (Fig. 2C). Moreover, depletion of RB1 induced apoptosis in serum-deprived cells, whereas depletion of both RB1 and PLD1 did not further promote apoptosis compared with that of PLD1 depletion, suggesting that RB1 repression may be involved in the downstream regulation of apoptosis by PLD1 depletion (Fig. 2D). Apparently, contradicting its role as a classical tumor suppressor protein, colorectal cancer cells retain the expression of RB1; they express high levels of RB1 compared with adjacent normal tissue, and loss or mutations of the *RB1* gene are rare (7, 21). Ablation of PLD1 in $Apc^{Min/+}$mice showed decreased level of RB1 in the intestinal tumors, whereas IEC-specific PLD1 overexpression recovered the levels of RB1 decreased in the tumor tissues from $Apc^{Min/+}Pld1^{-/-}$ mice (Fig. 2E). In addition, PLD1 inhibition suppressed the expression of RB1 in the tumor tissues from $Apc^{Min/+}$mice (Supplementary Fig. S3). Moreover, ablation of PLD1 in an AOM/DSS–induced mouse colon cancer model decreased the level of RB1 relative to that of control mice (Supplementary Fig. S4). Collectively, these data suggest that PLD1 inactivation–mediated apoptosis is intimately associated with downregulation of RB1.

Targeting PLD1 downregulates RB1 via miR-192 and -4465

We further examined how PLD1 regulates the level of RB1. Depletion and inhibition of PLD1 decreased the mRNA level of *RB1*, which was not affected by Akt1 and E2F1 depletion (Supplementary Fig. S5A). *RB1* is epigenetically silenced by hypermethylation of the CpG island within its promoter region (22). Histone methyltransferases, which bind to methylated CpG dinucleotides, not only recruit histone deacetylase, but also facilitate the methylation of H3 lysine 9, thereby reinforcing an inactive chromatin state (23). PLD1 inactivation did not affect DNA methylation (Supplementary Fig. S5B) or the binding of histone methyltransferase (H3K9me2) and acetyltransferase (H3K9ac) to the *RB1* promoter (Supplementary Fig. S5C). Moreover, targeting PLD1 did not affect the promoter activity of *RB1* (Supplementary Fig. S5D). miRNAs silence gene expression by binding to the 3′ untranslated regions (UTR) of target miRNAs, inhibiting their translation or marking them for degradation (24). Targeting of PLD1 abolished the luciferase activity of *RB1* 3′ UTR reporter (Fig. 3A), suggesting the involvement of miRNA in the regulation of RB1 expression by PLD1. miRNA microarray analysis showed that a total of 61 miRNAs displayed at least a 2-fold change in PLD1 inhibitor-treated DLD1 cells (GSE55771). On the basis of the bioinformatic approach, we found that miR-192 and -4465 upregulated by PLD1 inhibition have a putative target site in the 3′ UTR of RB1 that is conserved in various species (Fig. 3B). PLD1 inactivation significantly increased the expression of these

Published OnlineFirst October 28, 2016; DOI: 10.1158/0008-5472.CAN-15-3032

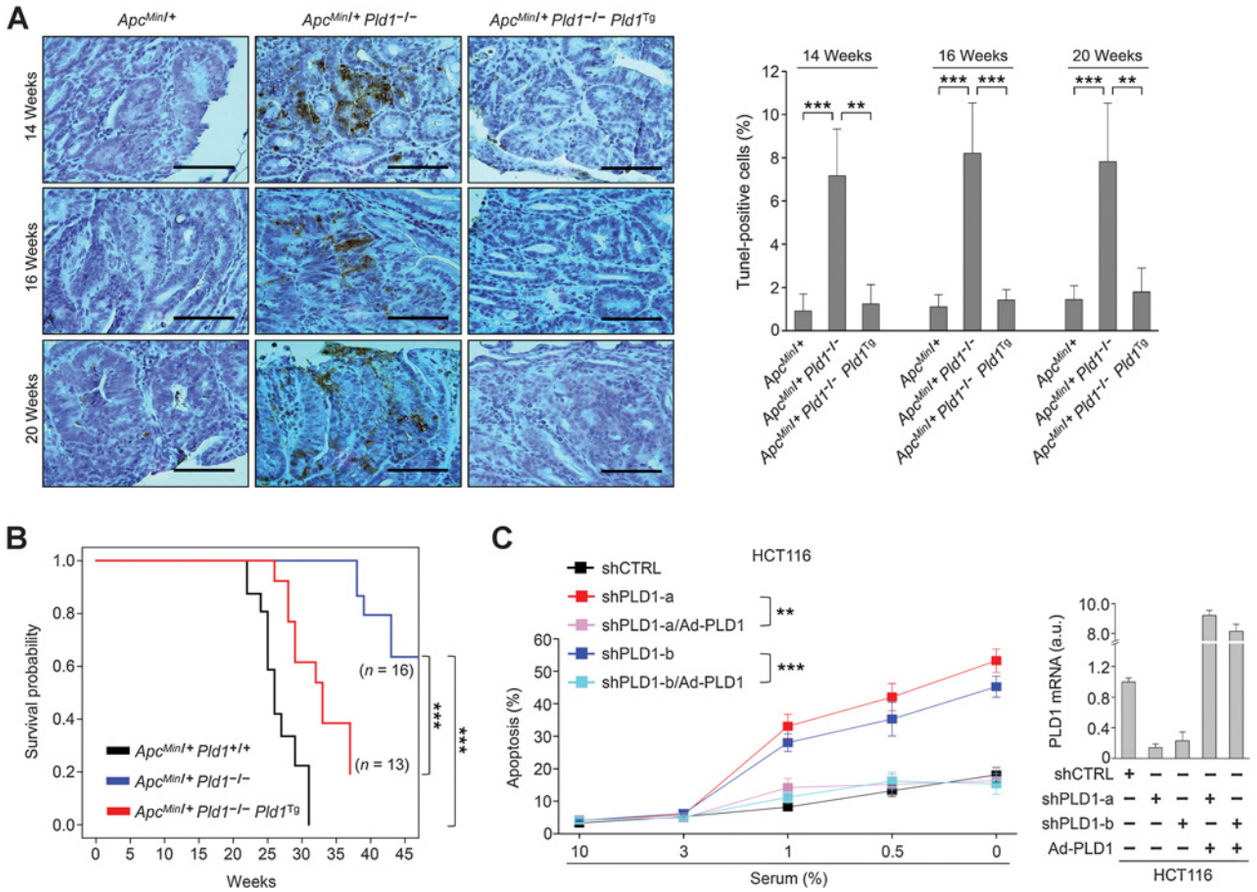

Figure 1.

PLD1 regulates apoptosis in $Apc^{Min/+}$ mice and colorectal cancer cells. **A,** TUNEL assay in distal small intestinal tumor tissues of the indicated mice (left). The TUNEL-positive cells were quantified as analyzed by the χ^2 test (right). $n = 6$ per group. **B,** The indicated mice were followed for long-term survival. Survival probability was analyzed using the Kaplan–Meier method, and the differences were evaluated using the log-rank test. **C,** Effect of PLD1 overexpression on PLD1 depletion–induced apoptosis under the indicated serum condition, as determined by an Annexin V apoptosis assay. Two-way ANOVA test was used. Results are shown as mean ± SEM and are representative of at least three independent experiments. **, $P < 0.01$; ***, $P < 0.001$.

miRNAs (Fig. 3C). Deletion of the putative binding sites of the miRNA recovered the decrease in luciferase activity of *RB1* 3′ UTR that occurred in response to PLD1 inactivation (Fig. 3D). Their precursor (pre)-miR inhibited *RB1* expression (Supplementary Fig. S6), whereas anti-miR recovered the luciferase activity of *RB1* 3′ UTR decreased by the targeting of PLD1 (Fig. 3E), suggesting that PLD1 inhibition downregulates *RB1* expression at the posttranscriptional level via miR-192 and -4465. Moreover, the expression of *RB1* showed a statistically inverse correlation with the expression of these miRNAs in colorectal cancer tissues (Fig. 3F), suggesting *in vivo* relevance. These data suggest that targeting PLD1 downregulates *RB1* via miR-192 and -4465.

Entangled pathways of Akt–TopBP1–E2F1–RB1 are involved in PLD1 inactivation–induced apoptosis

The E2F1 transcription factor can promote proliferation or apoptosis when activated and is a key downstream target of the RB1. The interaction of RB1 with E2F1 is known to inhibit E2F1 transactivation (25). Interestingly, PLD1 inactivation–induced apoptosis was suppressed by the depletion or ablation of E2F1, and this repression was recovered by the ectopic expression of E2F1 (Fig. 4A and B). The PI3K/Akt signaling pathway regulates E2F1 through the E2F1-interacting protein, TopBP1 (topoisomerase II β binding protein), which inhibits E2F1-dependent apoptosis (26). Phosphorylation of TopBP1 by Akt is crucial to interaction of TopBP1 with E2F1 and its repression. PLD1 inactivation greatly decreased the phosphorylation of Akt/TopBP1, RB1 expression, and the TopBP1–E2F1 and RB1–E2F1 interaction (Fig. 4C). In addition, the expression of PLD1 or ca-Akt1 increased the phosphorylation of TopBP1 and the interaction of TopBP1 with E2F1 (Fig. 4D). Targeting of PLD1 in $Apc^{Min/+}$and AOM/DSS mouse models reduced the phosphorylation of Akt, RB1 expression, and the interaction of E2F1 with RB1 or TopBP1 (Fig. 4E). IEC-specific PLD1 overexpression recovered the levels of p-Akt decreased in the tumor tissues from $Apc^{Min/+}Pld1^{-/-}$ mice (Fig. 4F). Moreover, IEC-specific PLD1 overexpression in $Apc^{Min/+}$ mice ($Apc^{Min/+}Pld1^{Tg}$) increased the levels of RB1 and p-Akt in the intestinal tumors, relative to $Apc^{Min/+}$ (Supplementary Fig. S7). In addition, PLD1 inhibition in the tumor tissues from $Apc^{Min/+}$or AOM/DSS mice decreased the level of p-Akt (Supplementary Fig. S8A and S8B).

Published OnlineFirst October 28, 2016; DOI: 10.1158/0008-5472.CAN-15-3032

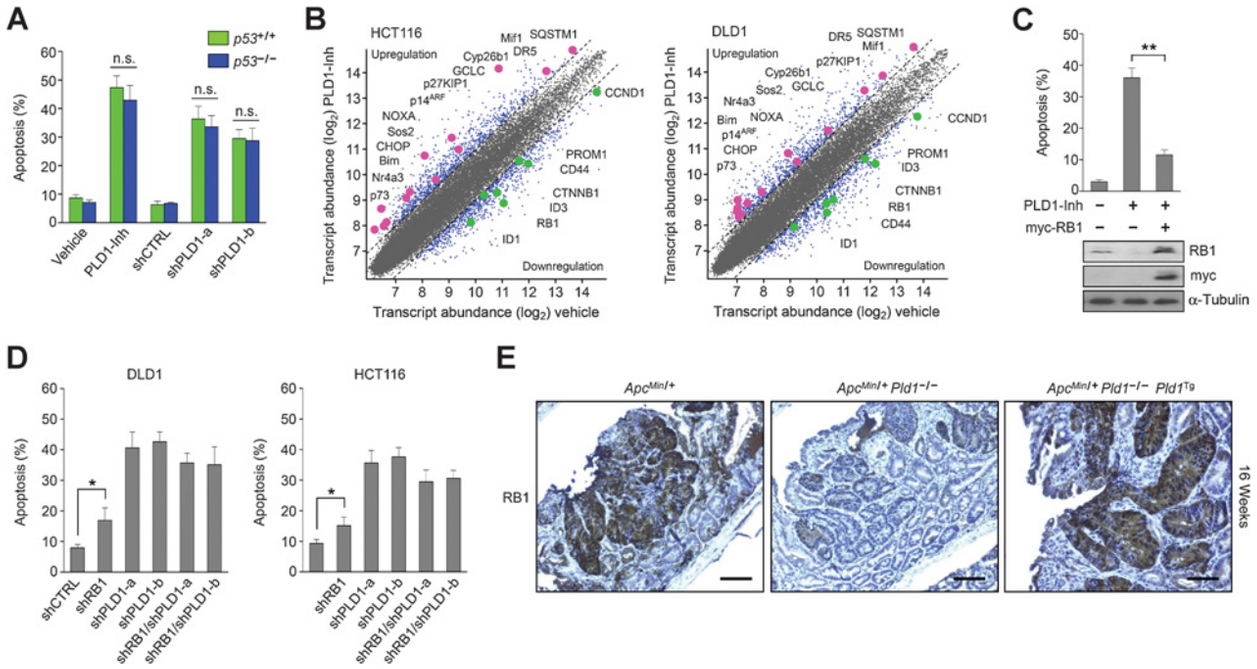

Figure 2.

PLD1 inactivation–induced apoptosis is associated with downregulation of RB1. **A,** Effect of p53 on PLD1 inactivation–induced apoptosis in $p53^{+/+}$ or $p53^{-/-}$HCT116 cells. n.s., not significant. **B,** Scatterplot of normalized mRNA expression analyzed by microarray in PLD1 inhibitor (VU0155069)–treated DLD1 cells. Data are log2 normalized. Some of the significantly up- or downregulated genes are indicated. Small blue dots, >2.0-fold deviation. Score of *y*-axis for gene ranking. **C,** Effect of RB1 on the PLD1 inhibitor–induced apoptosis in HCT116 cells. **D,** Effect of PLD1 depletion and/or RB1 on the apoptosis. **E,** IHC for RB1 in small intestinal tumor tissues of the indicated mice ($n = 6$/group). Scale bar, 100 μm. Two-way ANOVA test was used (**A**, **C**, and **D**). Results are shown as mean ± SEM and are representative of at least three independent experiments. *, $P < 0.05$; **, $P < 0.01$.

Taken together, these results suggest that both RB1–E2F1 and Akt–TopBP1–E2F1 signaling pathways are involved in PLD1-mediated apoptotic regulation.

PLD1 inactivation promotes the E2F1-dependent apoptotic program

Next, we examined potential downstream apoptotic effectors of the PLD1–E2F1 axis using microarray analysis in PLD1- and E2F1-depleted cells. Expression of some genes increased by PLD1 depletion was decreased by E2F1 depletion in two colorectal cancer cells (Fig. 5A). These genes are assumed to be targets of E2F1. A recent study identified a subset of E2F1 target genes required for E2F1-induced apoptosis that is specifically repressed by the PI3K/Akt signaling pathway (27). PLD1 inhibition significantly enhanced the expression of the proapoptotic E2F1 target genes (*NOXA*, *CHOP*, *Nr4a3*, *p27KIP1*, *p73*, and *Bim*) in serum-deprived HCT116 cells and that this enhancement was abolished by the depletion of E2F1 or expression of ca-Akt1 (Fig. 5B and C). Moreover, PLD1 inactivation in $Apc^{Min/+}$ mice enhanced the expression of the proapoptotic E2F1 target genes (Fig. 5D), suggesting *in vivo* relevance. Moreover, PLD1 inhibition enhanced the binding of E2F1 to promoters of its target genes, which was decreased by the expression of RB1 and ca-Akt1 (Fig. 5E). Furthermore, depletion of E2F1 target genes impaired PLD1 inhibition or E2F1-induced apoptosis under serum-deprived conditions (Fig. 5F; Supplementary Fig. S9). Taken together, these results suggest that PLD1 regulates the E2F1-dependent apoptotic program *in vivo* and *in vitro*.

PLD1 regulates apoptosis and the self-renewal capacity of CC-ICs via the miR-192/4465–RB1 axis and Akt pathway

We further investigated whether miR-192 and -4465 affect the E2F1 target gene expression and apoptosis. The anti-miR-192/4465 suppressed PLD1 inactivation–induced proapoptotic E2F1 target gene expression and apoptosis (Fig. 6A and B). Both pre-miR-192/4465 and Akt1 depletion further increased apoptosis under serum-deprived condition, compared with that of either expression (Fig. 6B), suggesting that both RB1 and Akt pathways are required for the promotion of apoptosis. We recently have reported that PLD1 is highly upregulated in the population of colon cancer–initiating cells (CC-IC; $CD133^+CD44^+$) and involved in self-renewal capacity. Interestingly, overexpression of RB1, ca-Akt1, or anti-miR-192/4465 significantly recovered $CD133^+CD44^+$ population and sphere-forming capacity decreased by PLD1 depletion (Fig. 6C and D). Although treatment of 5-fluorouracil and oxaliplatin, clinically used for colorectal cancer therapy, has a marginal effect on apoptosis of colorectal cancer cells under sphere culture, treatment of the drugs in PLD1-depleted cells increased the chemosensitivity (Fig. 6E). However, expression of RB1, ca-Akt1, and miR-192/4465 significantly reduced PLD1 depletion–induced chemosensitivity. PLD1-mediated cancer-initiating capacity is associated with upregulation of β-catenin and its target genes (12). Moreover, the decrease in expression of β-catenin and its target genes, in response to PLD1 depletion, was recovered by the overexpression of RB1, ca-Akt1, and anti-miR-192/4465 (Fig. 6F; Supplementary

Published OnlineFirst October 28, 2016; DOI: 10.1158/0008-5472.CAN-15-3032

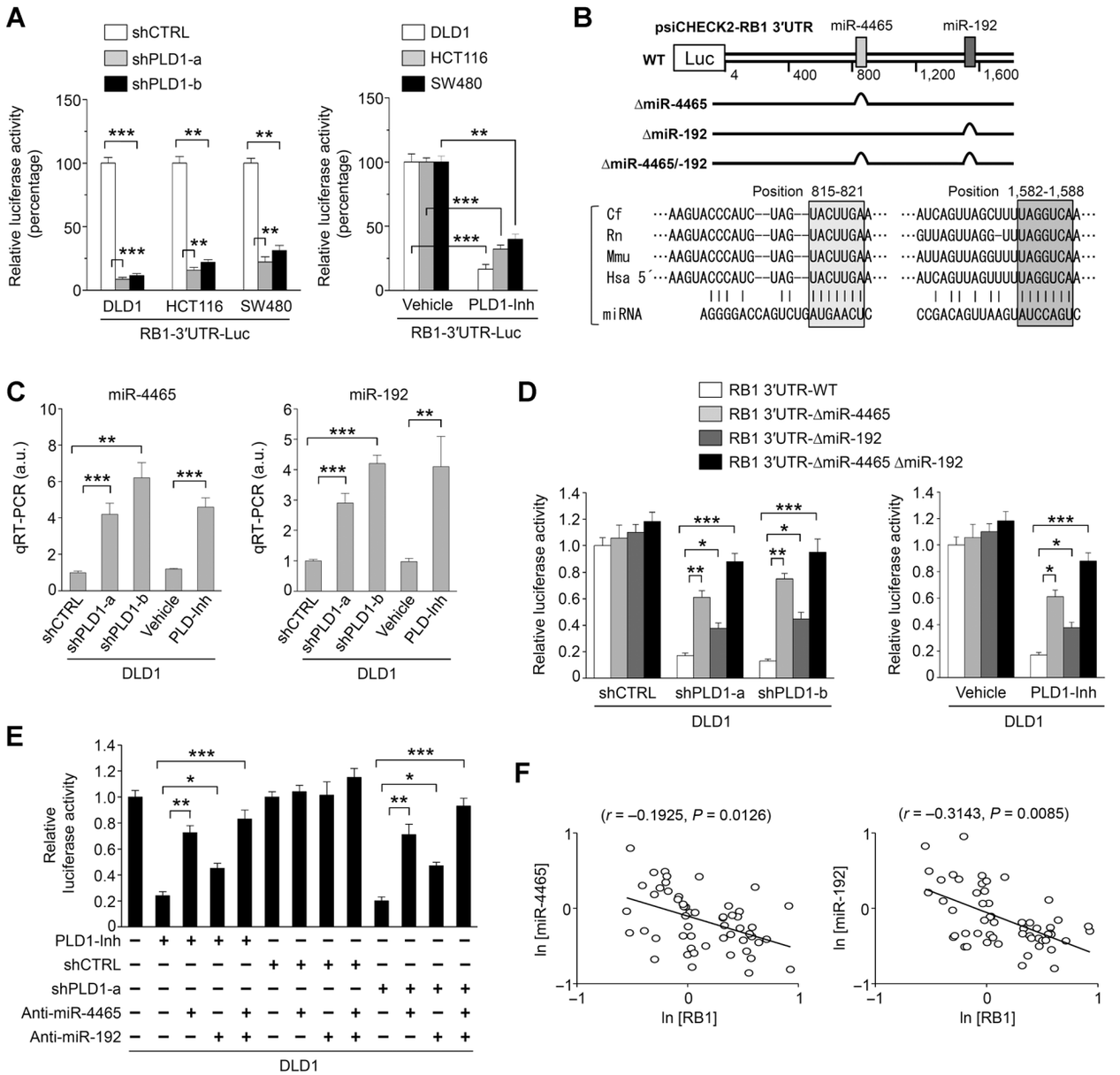

Figure 3.

Targeting PLD1 downregulates RB1 via miR-192 and -4465. **A,** Effect of depletion (left) and inhibition (right) of PLD1 on the luciferase activity of *RB1* 3′ UTRs. a.u., arbitrary units. **B,** Schematic representation of luciferase constructs of *RB1* 3′ UTR and highly conserved and predicted binding sites for the seed sequences of the miRNA. **C,** qRT-PCR analysis of miR-4465 and miR-192 under the indicated condition. **D,** Effect of PLD1 inactivation on the luciferase activity of the indicated *RB1* 3′ UTR. **E,** Effect of anti-miR-4465/192 on PLD1 inactivation–mediated suppression of *RB1* 3′ UTR luciferase activity. **F,** Inverse correlation of RB1 and the indicated miRNA expression in the tumor tissues from colorectal cancer patients. Spearman correlation coefficient (*r*) is provided with its statistical significance. Black lines, best-fit curves. A paired *t* test was used (**A** and **C**–**E**). Results are representative of at least three independent experiments and are shown as mean ± SEM. *, $P < 0.05$; **, $P < 0.01$; ***, $P < 0.001$.

Fig. S10). Furthermore, their overexpression recovered the binding of β-catenin to the promoter of its target genes, which was decreased by PLD1 depletion (Fig. 6G). Taken together, these results suggest that PLD1 regulates apoptosis and the self-renewal capacity of CC-ICs via the miR-192/4465–RB1 axis and Akt pathway.

Low PLD1 level, coupled with high expression of E2F1 targets and low level of RB1 expression, is associated with increased survival of colorectal cancer patients

We next attempted to demonstrate the physiologic relevance of the relationship of PLD1 level with the expression of E2F1 target genes, RB1, and miR-192/4465. The mRNA expression in

Published OnlineFirst October 28, 2016; DOI: 10.1158/0008-5472.CAN-15-3032

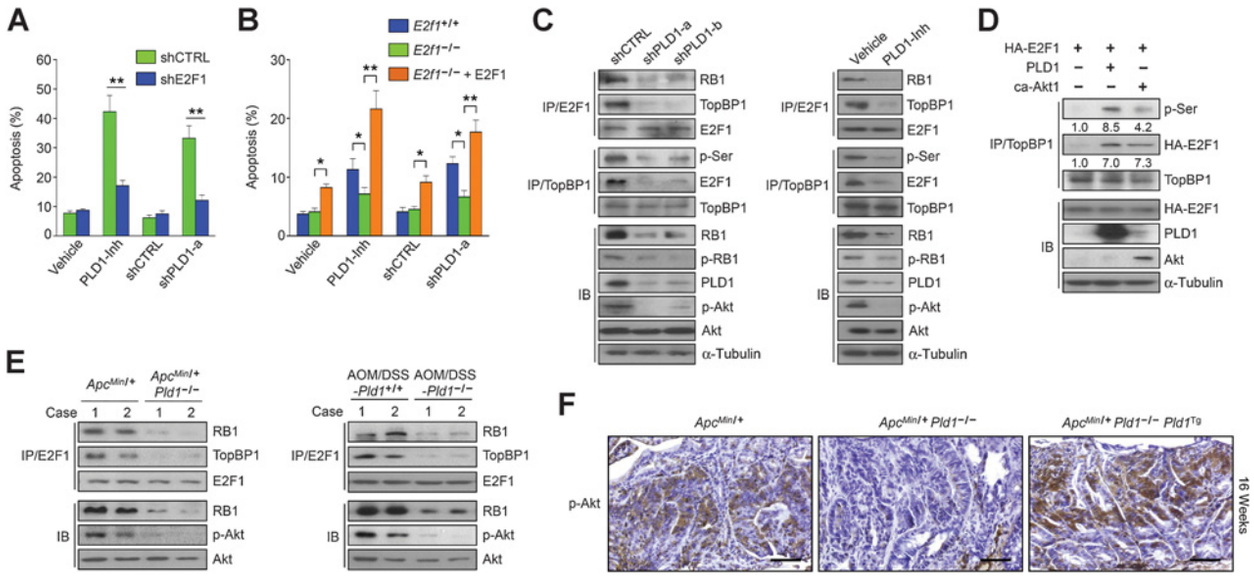

Figure 4.

Entangled pathways of Akt–TopBP1–E2F1–RB1 are involved in PLD1 inactivation–induced apoptosis. **A** and **B,** Effect of E2F1 on PLD1 inactivation–induced apoptosis in HCT116 (**A**) and MEF (**B**) cells under 1% serum condition. Two-way ANOVA test was used. **C,** Effect of PLD1 on the interaction and expression of the indicated proteins in PLD1-depleted cells (left) and PLD1 inhibitor–treated cells (right). **D,** Effect of E2F1 and Akt1 on the interaction and expression of the indicated proteins. **E,** Expression and interaction of the indicated proteins in the tumor tissues from $Apc^{Min/+}$ or $Apc^{Min/+}Pld1^{-/-}$ mice ($n = 7$ mice/group; left) and AOM/DSS in $Pld1^{+/+}$ or $Pld1^{-/-}$ mice ($n = 8$ mice/group; right). **F,** IHC for p-Akt in the tumor tissues of the indicated mice ($n = 6$/group). Scale bar, 100 μm. Results are shown as mean ± SEM and are representative of at least three independent experiments. *, $P < 0.05$; **, $P < 0.01$.

55 colorectal cancer tissues exhibited elevated expression of RB1, reduction of proapoptotic E2F1 target genes, miR-4465, and miR-192 (Fig. 7A), compared with that of normal tissues. Moreover, expression of PLD1 and the E2F1 target genes showed a strong negative correlation, whereas a positive correlation of PLD1 with RB1 was noted in colorectal cancer tissues as analyzed by qRT-PCR (Fig. 7B). miR-192, but not miR-4465, showed a significant negative correlation with PLD1 level in colorectal cancer tissues (Fig. 7B). Consistently, elevated expression of PLD1 in colorectal cancer was found to be positively correlated with levels of RB1 and p-Akt, but negatively correlated with the E2F1 targets as analyzed by IHC (Fig. 7C). The tumors were interpreted as low when immunostaining was weak, as in the corresponding normal colonic mucosa, or when immunopositive cells represented <10% of the cancer cells. Factors of multivariate variables, the basic features, and the protein group using Cox proportional hazards model, show that survival difference between PLD1/p27KIP1/Bim/NOXA expression groups are, in a statistical significance, associated with tumor stage (Supplementary Table S4), but not with gender, organ, and age. Fitted survival function for the protein groups, in which tumor stage was considered, shows that a low level of PLD1 with high expression of E2F1 targets ($PLD1^{L}/p27KIP1^{H}$ $PLD1^{L}/Bim^{H}$, and $PLD1^{L}/NOXA^{H}$) was significantly correlated with higher overall survival of colorectal cancer patients, and vice versa (Fig. 7D; Supplementary Fig. S11). Taken together, these data support an intimate association of PLD1 expression with levels of the E2F1 target genes in the survival of colorectal cancer patients and suggest a potential value of PLD1 and E2F1 targets as prognostic biomarkers and therapeutic targets of colorectal cancer.

Discussion

In the current study, we demonstrate that PLD1 has a previously unrecognized role in regulating E2F1-dependent apoptosis, which is entangled with the RB1 and Akt/TopBP1 pathways and emerges as a potential therapeutic target in colorectal cancer. The numerous signaling molecules affecting cancer cells operate as nodes and branches of elaborate integrated circuits that are reprogrammed derivatives of the circuits operating in normal cells (16). Our findings show that PLD1 orchestrates the crosstalk between RB1–E2F1 and Akt–TopBP1 signaling pathways and contributes to apoptotic regulation and self-renewal of colorectal cancer. Targeting these signaling networks is particularly attractive, as almost all human cancers exhibit alterations in these pathways; however, key modulators and the mechanism underlying the functional interaction among the signaling circuits in colorectal cancer remains elusive. Our findings that PLD1-mediated apoptotic regulation occurs through E2F1 and RB1, but not p53, suggest the possibility that PLD1 might be a new regulator of RB1–E2F1 signaling circuits in colorectal cancer cells. PLD1 inactivation increases the transactivation of E2F1 and its apoptotic program via the suppression of both RB1 and Akt–TopBP1 pathways. Genetic and pharmacologic targeting of PLD1 in $Apc^{Min/+}$ mice greatly increased the expression of proapoptotic E2F1 target genes, which ultimately is involved in the attenuation of intestinal tumorigenesis. Indeed, a variety of cancer-relevant molecules and signaling pathways intersect with the Wnt pathway and may modulate it. We recently demonstrated that the inactivation of PLD1 downregulates β-catenin expression via E2F1-induced miR-4496 upregulation (12). Ultimately, PLD1

Published OnlineFirst October 28, 2016; DOI: 10.1158/0008-5472.CAN-15-3032

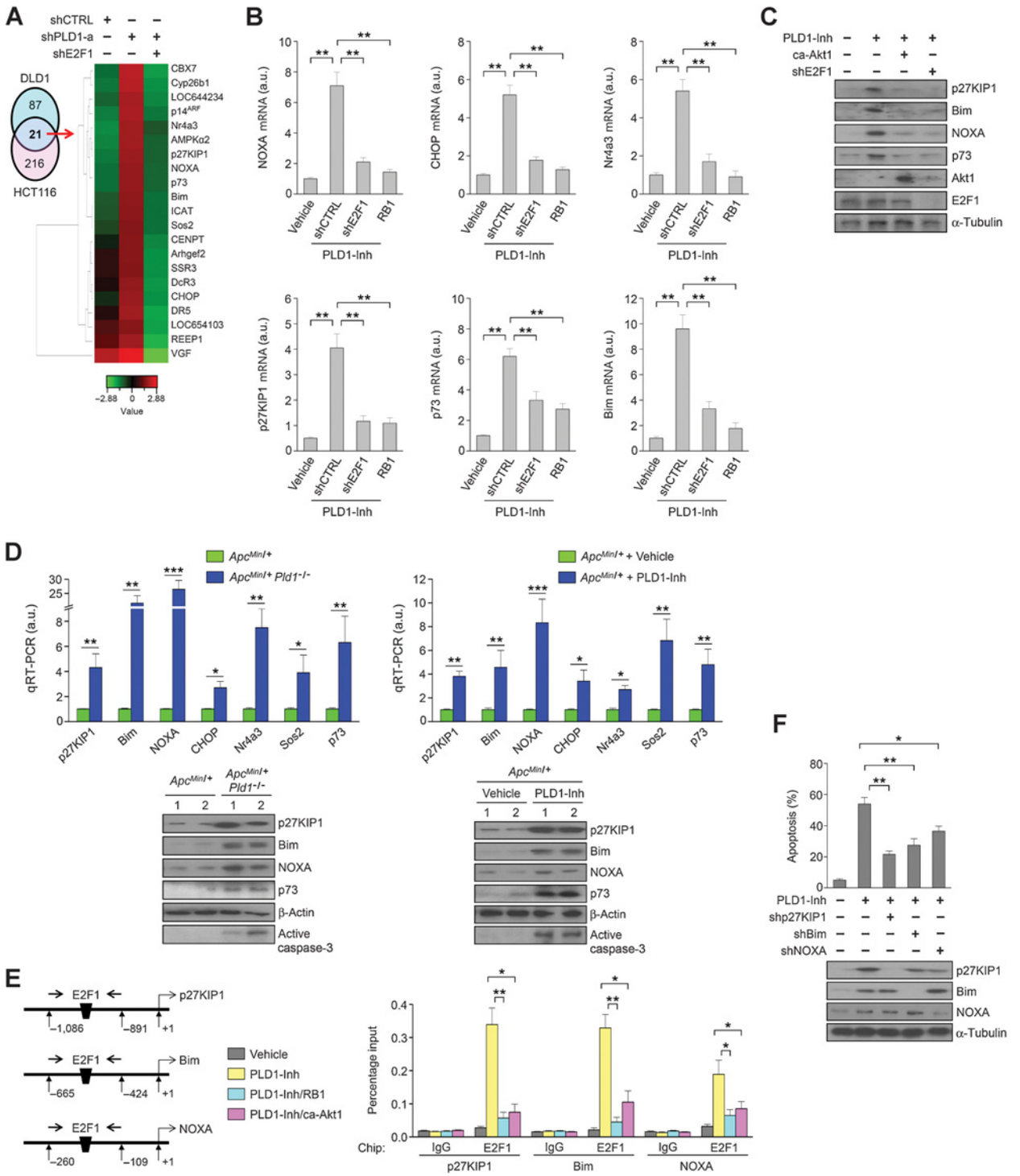

Figure 5.

PLD1 inactivation promotes the E2F1-dependent apoptotic program. **A,** Cluster analysis of mRNA commonly repressed by E2F1 depletion among all genes upregulated by PLD1 depletion. **B,** Effect of E2F1 or RB1 depletion on PLD1 inhibitor–induced E2F1 proapoptotic target gene expression. **C,** Effect of Akt1 overexpression and E2F1 depletion on the PLD1 inhibitor–induced E2F1 proapoptotic target gene expression. **D,** qRT-PCR (top) and immunoblot (bottom) analysis of tumor tissues from the indicated mice. a.u., arbitrary units. **E,** Schematic representation of E2F1-binding elements in the promoter regions of p27KIP1, Bim, and NOXA. Chromatin immunoprecipitation assays for the binding of E2F1 to the indicated promoters by transduction with RB1 and ca-Akt1 with treatment of PLD1 inhibitor in DLD1 cells. **F,** Effect of depletion of p27KIP1, Bim, and NOXA on PLD1 inhibitor–induced apoptosis (top) and immunoblot analysis (bottom). A paired *t* test was used (**A**, **B**, and **D–F**). Results are representative of at least three independent experiments and are shown as mean ± SEM. *, $P < 0.05$; **, $P < 0.01$; ***, $P < 0.001$.

Published OnlineFirst October 28, 2016; DOI: 10.1158/0008-5472.CAN-15-3032

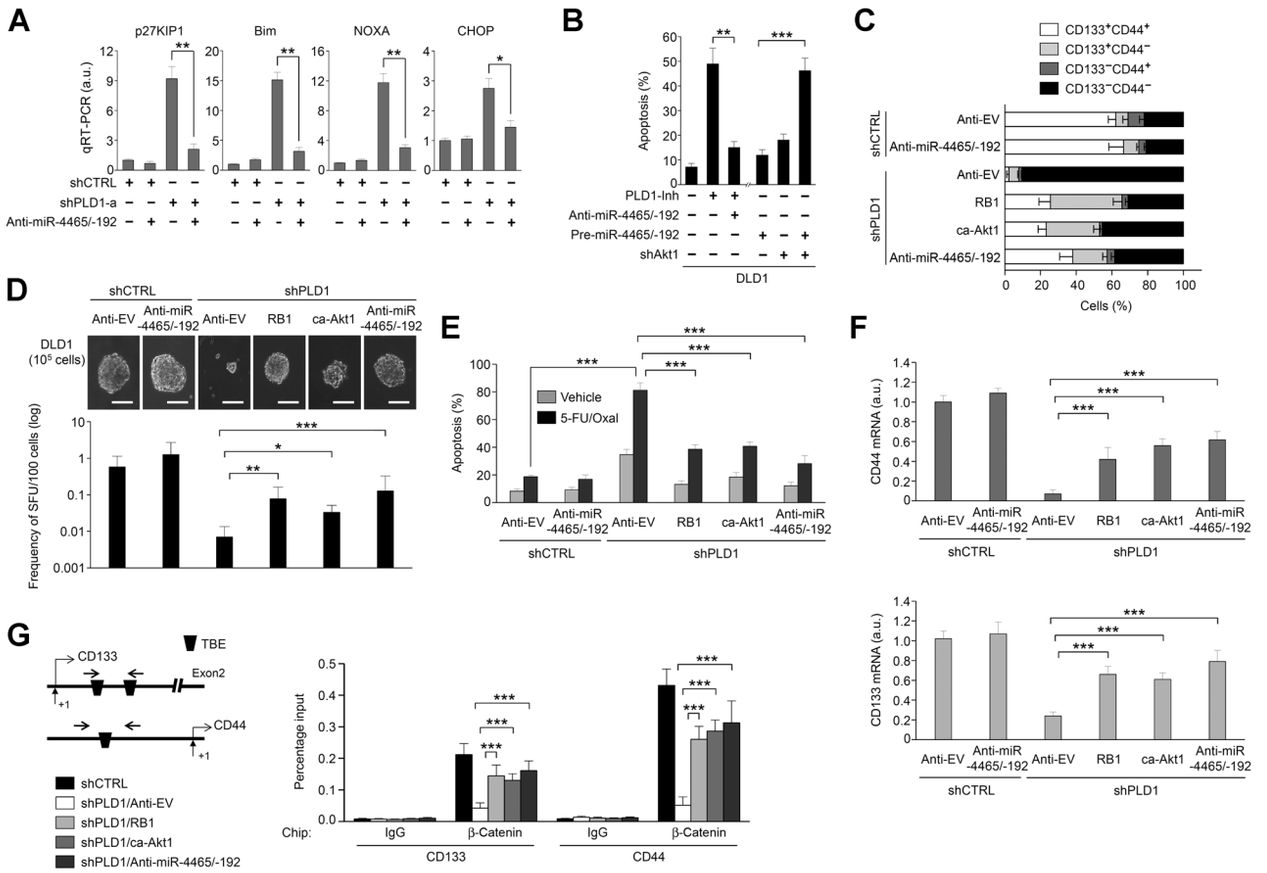

Figure 6.

PLD1 regulates apoptosis and the self-renewal capacity of CC-ICs via the miR-192/4465–RB1 axis and Akt pathway. **A,** Effect of anti-miR-4465/192 on the expression of proapoptotic E2F1 target genes. a.u., arbitrary units. **B,** Effect of the indicated anti-miR or pre-miR and/or Akt1 depletion on PLD1 inhibitor–induced apoptosis. **C,** Representative flow cytometric profiles of CD44 and CD133 expression by transduction with lentiviruses of the indicated constructs in PLD1-depleted DLD1. **D,** Frequency of secondary sphere-forming units (SFU) by transduction with RB1, ca-Akt1, or anti-miR in PLD1-depleted cells, as determined by *in vitro* limiting dilution assays. Scale bar, 50 μm. **E,** After PLD1-depleted cells were expressed with the indicated constructs under sphere culture condition and treated with 5-fluorouracil (5-FU, 50 μg/ml) and oxaliplatin (Oxal, 100 μmol/L), the percentage of apoptotic cells was measured. Effect of RB1, ca-Akt1, or anti-miR on the expression of CD133 and CD44 suppressed by PLD1 depletion under sphere culture condition. **G,** Effect of RB1, ca-Akt1, or anti-miR on the binding of β-catenin/TCF to the promoter of CD133 and CD44 genes. A paired *t* test was used (**A**, **B**, and **D–G**). Results are shown as mean ± SEM and are representative of at least three independent experiments. *, $P < 0.05$; **, $P < 0.01$; ***, $P < 0.001$.

regulates tumor-initiating capacity through the E2F1–miR-4496–β-catenin signaling axis (11). miR-4496 is a new target of E2F1 and a crucial node responsible for mediation of the cross-talk between E2F1 and Wnt/β-catenin signaling. PLD1 inactivation increases the expression of PI3K-repressed E2F1 target genes via both downregulation of RB1 and inhibition of the PI3K/Akt1–TopBP1 pathway, which is followed by activation of the apoptotic program and suppression of Wnt/β-catenin signaling. E2F1 can function as both a tumor suppressor and an oncogene under different conditions (28). Unlike other human cancers, in most colorectal cancers, although Wnt/β-catenin signaling is activated, E2F1 activity is kept at a low level because there are no mutations in RB1 (29). Moreover, instead of acting as an oncogene, E2F1 in human colorectal cancer may function as a tumor suppressor (30). It has long been known that *RB1* in colon carcinoma is not mutated, but overexpressed, and even amplified (7, 21). Thus, in the context of colorectal cancer, RB1 is more likely to act as an oncoprotein than a tumor suppressor. In this regard, strategies focused on the control of E2F1 proteins hold particular promise, as activation of E2F activity is the ultimate consequence of deregulation of the RB1 pathway. E2F1 activity is negatively regulated by PLD1; accordingly, retaining *RB1* and amplifying PLD1 may enable colorectal cancer cells to select for mechanisms that limit the activity of E2F1 and tip the balance toward β-catenin–driven proliferation conditions that suppress E2F1 and enhance the activity of β-catenin. Interestingly, PLD1 inactivation reduced the expression of RB1 via miR-192 and -4465; thus, downregulation of RB1 by targeting PLD1 may release active E2F1 and induce E2F1 transactivation. This is the first evidence that PLD1 regulates the expression of β-catenin and RB1 at the posttranscriptional level via the miRNA; accordingly, PLD1 inactivation regulates E2F1-mediated apoptosis and cancer-initiating capacity by modulating RB1 expression and Akt pathway, E2F1 transactivation, and β-catenin signaling. Interestingly, the survival probability between PLD1 and the E2F1 target protein–expressed patient groups was significantly associated with tumor stage,

Published OnlineFirst October 28, 2016; DOI: 10.1158/0008-5472.CAN-15-3032

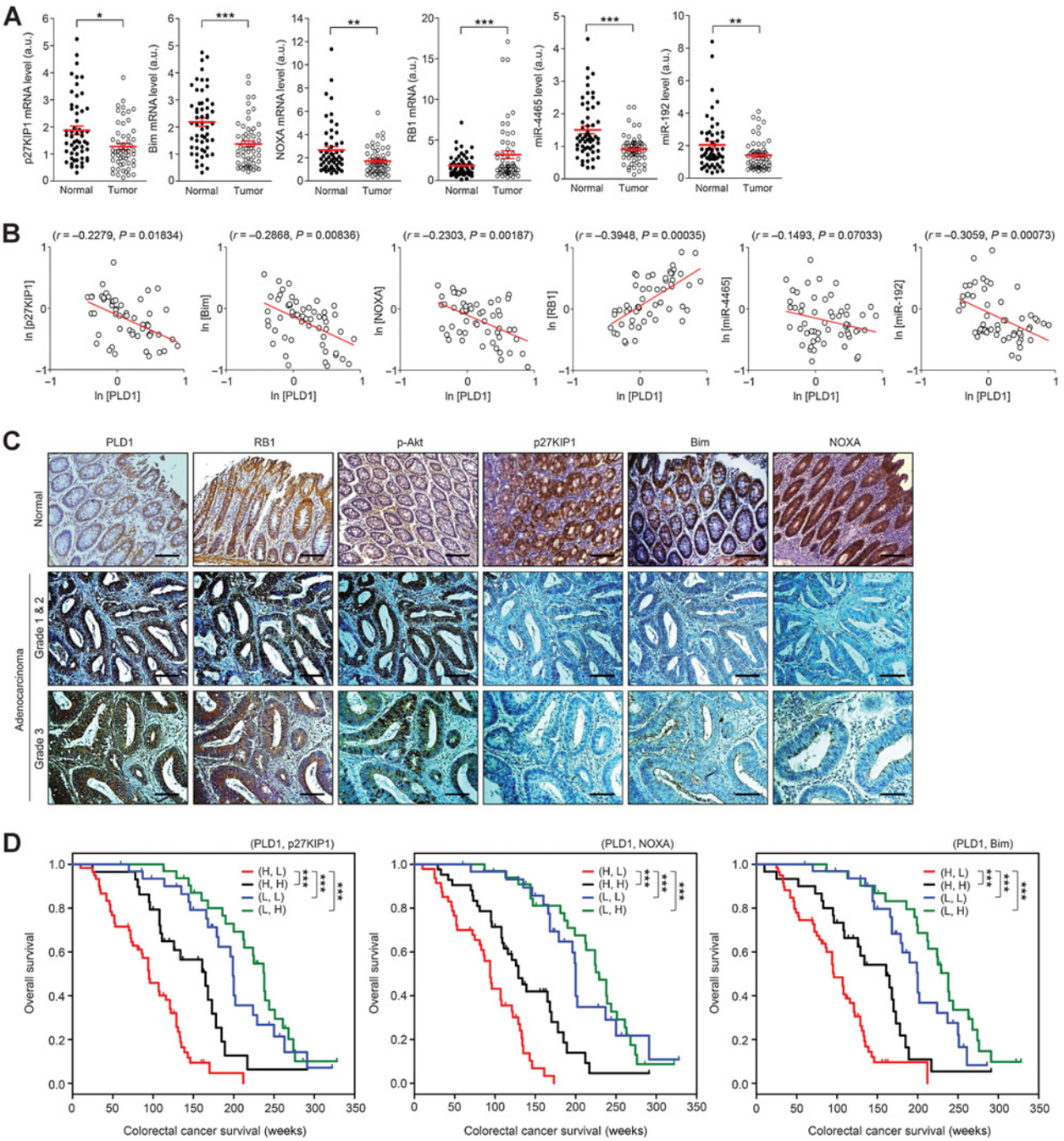

Figure 7.

Expression of PLD1 and proapoptotic E2F1 target genes is associated with survival of colorectal cancer patients. **A,** Relative expression of the indicated genes in 55 pairs of tumor and adjacent normal tissues from colorectal cancer patients was measured by qRT-PCR. Two-way ANOVA test was used. a.u., arbitrary units. Results are representative of at least two independent experiments and are shown as mean ± SEM. *, $P < 0.05$; **, $P < 0.01$; ***, $P < 0.001$. **B,** In 55 tumor tissues from colorectal cancer patients, there was inverse correlation of PLD1 with E2F1 target gene expression or miR-192 and a positive correlation of PLD1 with RB1 mRNA expression. Spearman correlation coefficient (r) is provided with its statistical significance (P). Red lines, best-fit curves. **C,** Immunohistochemical staining in tumor and adjacent normal tissues from colorectal cancer patients. Scale bar, 100 μm. **D,** Correlation with survival when patient specimens are segregated according to immunoreactivity of PLD1 with E2F1 target (p27KIP1, Bim, NOXA). Kaplan–Meier survival curves of colorectal cancer patients ($n = 153$) are presented. L, low expression; H, high expression. The differences were evaluated using log-rank test. ***, $P < 0.001$.

suggesting that the proteins might be potential prognostic biomarkers in colorectal cancer patients. Collectively, our findings demonstrate that PLD1 plays a crucial role in apoptosis and cancer-initiating capacity, via regulation of the cross-talk among RB1–E2F1, PI3K/Akt–TopBP1, and Wnt/β-catenin pathways. These results provide a missing link between the signaling networks mediating cancer and may fill the gap in current knowledge regarding how the complexity of these pathways is delicately regulated in cancer. Considering the highly complex interactions among cancer-relevant pathways, targeting these pathways by PLD1 inhibition might be an effective therapy for the treatment of colorectal cancer.

Disclosure of Potential Conflicts of Interest

No potential conflicts of interest were disclosed.

Authors' Contributions

Conception and design: D.W. Kang, D.S. Min
Development of methodology: D.W. Kang, D.S. Min
Acquisition of data (provided animals, acquired and managed patients, provided facilities, etc.): D.W. Kang, S.W. Lee, W.C. Hwang, Y.-A. Suh, K.-Y. Choi, D.S. Min
Analysis and interpretation of data (e.g., statistical analysis, biostatistics, computational analysis): D.W. Kang, S.W. Lee, W.C. Hwang, B.H. Lee, Y.-S. Choi, D.S. Min
Writing, review, and/or revision of the manuscript: D.W. Kang, S.W. Lee, K.-Y. Choi, D.S. Min
Administrative, technical, or material support (i.e., reporting or organizing data, constructing databases): D.W. Kang, S.W. Lee, Y.-A. Suh, D.S. Min
Study supervision: D.S. Min

Grant Support

This study was supported by a National Research Foundation of Korea(NRF) grant funded by the Korean government (NRF-2015R1A2A1A05001884), a Translational Research Center for Protein Function Control grant (2016R1A5A11004694), a National R&D Program for Cancer Control grant from the Ministry for Health, Welfare, and Family Affairs (Republic of Korea; 0920050), and Korean Health Technology R&D Project, Ministry of Health & Welfare, Republic of Korea (HI06C0868).

The costs of publication of this article were defrayed in part by the payment of page charges. This article must therefore be hereby marked *advertisement* in accordance with 18 U.S.C. Section 1734 solely to indicate this fact.

Received November 5, 2015; revised October 10, 2016; accepted October 23, 2016; published OnlineFirst October 28, 2016.

References

1. Classon M, Harlow E. The retinoblastoma tumor suppressor in development and cancer. Nat Rev Cancer 2002;2:910–7.
2. Rowland BD, Bernards R. Re-evaluating cell-cycle regulation by E2Fs. Cell 2006;127:871–4.
3. Gope ML, Chun M, Gope R. Comparative study of the expression of RB and p53 genes in human colorectal cancers, colon carcinoma cell lines and synchronized human fibroblasts. Mol Cell Biochem 1991;107:55–63.
4. Morris EJ, Ji JY, Yang F, Di Stefano L, Herr A, Moon NS, et al. E2F1 represses β-catenin transcription and is antagonized by both pRB and CDK8. Nature 2008;455:552–6.
5. Hughes TA, Brady HJ. Cross-talk between pRb/E2F and Wnt/beta-catenin pathways: E2F1 induces axin2 leading to repression of Wnt signalling and to increased cell death. Exp Cell Res 2005;303:32–46.
6. van de Wetering M, Sancho E, Verweij C, de Lau W, Oving I, Hurlstone A, et al. The beta-catenin/TCF-4 complex imposes a crypt progenitor phenotype on colorectal cancer cells. Cell 2002;111:241–50.
7. Firestein R, Bass AJ, Kim SY, Dunn IF, Silver SJ, Guney I, et al. CDK8 is a colorectal cancer oncogene that regulates β-catenin activity. Nature 2008;455:547–51.
8. Polager S, Ginsberg D. p53 and E2f: partners in life and death. Nat Rev Cancer 2009;9:738–48.
9. Kang DW, Choi KY, Min DS. Phospholipase D meets Wnt signaling: a new target for cancer therapy. Cancer Res 2011;71:293–7.
10. Kang DW, Lee SH, Yoon JW, Park WS, Choi KY, Min DS. Phospholipase D1 drives a positive feedback loop to reinforce the Wnt/β-catenin/TCF signaling axis. Cancer Res 2010;70:4233–42.
11. Kang DW, Choi CY, Cho YH, Tian H, Paolo GD, Choi KY, et al. Targeting phospholipase D1 attenuates intestinal tumorigenesis by controlling β-catenin signaling in cancer-initiating cells. J Exp Med 2015;212:1219–37.
12. Selvy PE, Lavieri RR, Lindsley CW, Brown HA. Phospholipase D: enzymology, functionality, and chemical modulation. Chem Rev 2011;12:6064–119.
13. Su W, Chen Q, Frohman MA. Targeting phospholipase D with small molecule inhibitors as a potential therapeutic approach for cancer metastasis. Future Oncol 2009;5:1477–86.
14. Kang DW, Park MK, Oh HJ, Lee DG, Park SH, Choi KY, et al. Phospholipase D1 has a pivotal role in interleukin-1β-driven chronic autoimmune arthritis through regulation of NF-κB, hypoxia-inducible factor 1α, and FoxO3a. Mol Cell Biol 2013;33:2760–72.
15. Hu Y, Smyth GK. ELDA: extreme limiting dilution analysis for comparing depleted and enriched populations in stem cell and other assays. J Immunol Methods 2009;347:70–8.
16. Hanahan D, Weinberg RA. Hallmarks of cancer: the next generation. Cell 2011;144:646–74.
17. Foster DA, Xu L. Phospholipase D in Cell Proliferation and Cancer. Mol Cancer Res 2003;1:789–800.
18. Kim J, Lee YH, Kwon TK, Chang JS, Chung KC, Min DS. Phospholipase D prevents etoposide-induced apoptosis by inhibiting the expression of early growth response-1 and phosphatase and tensin homologue deleted on chromosome 10. Cancer Res 2006;66:784–93.
19. Hui L, Abbas T, Pielak RM, Joseph T, Bargonetti J, Foster DA. Phospholipase D elevates the level of MDM2 and suppresses DNA damage-induced increases in p53. Mol Cell Biol 2004;24:5677–86.
20. Lyo D, Xu L, Foster DA. Phospholipase D stabilizes HDM2 through an mTORC2/SGK1 pathway. Biochem Biophys Res Commun 2010;396:562–5.
21. Lai PS, Cheah PY, Kadam P, Chua CL, Lie DK, Li HH, et al. Overexpression of RB1 transcript is significantly correlated with 13q14 allelic imbalance in colorectal carcinomas. Int J Cancer 2006;119:1061–6.
22. Greger V, Debus N, Lohmann D, Höpping W, Passarge E, Horsthemke B. Frequency and parental origin of hypermethylated RB1 alleles in retinoblastoma. Hum Genet 1994;94:491–6.
23. Fuks F, Hurd PJ, Deplus R, Kouzarides T. The DNA methyltransferases associate with HP1 and the SUV39H1 histone methyltransferase. Nucleic Acids Res 2003;31:2305–12.
24. Pauli A, Rinn JL, Schier AF. Non-coding RNAs as regulators of embryogenesis. Nat Rev Genet 2011;12:136–49.
25. Chellappan SP, Hiebert S, Mudryj M, Horowitz JM, Nevins JR. The E2F transcription factor is a cellular target for the RB protein. Cell 1991;65:1053–61.
26. Liu K, Paik JC, Wang B, Lin FT, Lin WC. Regulation of TopBP1 oligomerization by Akt/PKB for cell survival. EMBO J 2006;25:4795–807.
27. Hallstrom TC, Nevins JR. Specificity in the activation and control of transcription factor E2F-dependent apoptosis. Proc Natl Acad Sci USA 2003;100:10848–53.
28. Trimarchi JM, Lees JA. Sibling rivalry in the E2F family. Nat Rev Mol Cell Biol 2002;3:11–20.
29. Nevins JR. The RB/E2F1 pathway and cancer. Human Mol Genet 2001;10:699–703.
30. Bramis J, Zacharatos P, Papaconstantinou I, Kotsinas A, Sigala F, Korkolis DP, et al. E2F-1 transcription factor immunoexpression is inversely associated with tumor growth in colon adenocarcinomas. Anticancer Res 2004;24:3041–7.

Cancer Research
The Journal of Cancer Research (1916–1930) | The American Journal of Cancer (1931–1940)

AACR American Association for Cancer Research

Phospholipase D1 Acts through Akt/TopBP1 and RB1 to Regulate the E2F1-Dependent Apoptotic Program in Cancer Cells

Dong Woo Kang, Shin Wha Lee, Won Chan Hwang, et al.

Cancer Res 2017;77:142-152. Published OnlineFirst October 28, 2016.